

# Chapter 3

## HYPERFINE INTERACTION STUDIES IN DILUTE MAGNETIC SEMICONDUCTOR

Fe-Sb-Se

### Contents

<b>3. Hyperfine interaction studies in dilute magnetic semiconductor Fe-Sb-Se</b>	
3.1 Introduction	56
3.2 Sample Preparation	58
3.3 Experimental Results	59
3.3.1 Mossbauer measurements	59
3.3.2 Hall Measurements	74
3.3.3 X-Ray diffraction studies	76
3.3.4 Magnetoresistance measurements	79
3.3.5 A.C.Susceptibility measurements	83
3.4 Summary	85
References	86

## HYPERFINE INTERACTION STUDIES IN DILUTE MAGNETIC SEMICONDUCTOR Fe-Sb-Se

### 3.1 Introduction

Substitution of very small concentration of transitional metal impurities into the host lattice of semiconducting compounds and/or non magnetic metals makes Dilute Magnetic Semiconductors (DMS) or Dilute magnetic alloys. Some of the examples of such alloys are II-VI and IV-VI based  $\text{Cd}_{1-x}\text{Mn}_x\text{Te}$ ,  $\text{Zn}_{1-x}\text{Mn}_x\text{Te}$ ,  $\text{Ge}_{1-x}\text{Mn}_x\text{Te}$ ,  $\text{Zn}_{1-x}\text{Fe}_x\text{Se}$  etc [1-5]. These materials possess exotic physical and opto-electronic properties. The potential application of these materials is in Opto-electronic devices, MRAM and SPINTRONCS technology. They exhibit magnetic as well as semiconducting properties. However the curie temperatures of such materials were observed much below room temperature. But various efforts were put to raise the curie temperature upto and above room temperature. For this a better understanding of the magnetic interaction and transport properties of these materials are essential. Recently in magnetically doped III-V based ZnO [6], GaN [7] and  $\text{TiO}_2$  [8], the curie temperature was found to be 280, 250 and 400K respectively. In ternary compounds like  $(\text{Cd}_{0.8}\text{Mn}_{0.2})\text{GeP}_2$  [9],  $(\text{Zn}_{0.8}\text{Mn}_{0.2})\text{SnAs}_2$  [10] and  $(\text{Zn}_{0.94}\text{Mn}_{0.06})\text{GeP}_2$  [11], the ferromagnetic ordering was observed at 320, 329 and 312K respectively.

The cause of ferromagnetism in such systems was well explained by Dietl. et. al. [12] & Matsukara et.al [13]. They proposed the carrier induced ferromagnetism at room temperature caused by exchange interaction between delocalized carriers

and localized spins known to be RKKY type of interactions. These carrier densities are brought into the systems by doping magnetic ion concentration. Hence on increasing the carrier densities the exchange interactions can be enhanced. But this may lead to higher magnetic ion concentration, which may cause the formation of magnetic phases into the host material. For examples, MnN and MnAs are the phases observed in GaMnN and GaMnAs systems.

However if the dopant magnetic ion concentration is kept low and constant and the variation of charge carrier density can be brought about by varying the concentration of the anion in the semiconductor (B site in AB type), it will be still possible to keep the system in dilute limit and yet may be possible to bring about ferromagnetism at room temperature. Most of the earlier studies have kept the A and B site concentration constant at the stoichiometric proportions. Thus it will be interesting to study the effect of varying B site concentration in the II-VI, III-V, IV-VI or V-VI based systems. Thus keeping the A site material as the base a continuous alloy is made by varying the concentration of B component.

In this Chapter, we discuss the variation of chalcogenide concentration Se in the host lattice Sb and keeping the magnetic ion Fe concentration constant and in very dilute limit. In such a dilute system  $Sb_{1-x-y}Fe_xSe_y$  to test the magnetic ordering, the usual bulk solid state techniques of magnetization measurements may not be very sensitive. Measuring the hyperfine magnetic fields at the nucleus of the magnetic ions is a much more sensitive technique and hence the nuclear hyperfine interaction techniques like MS and TDPAC can be used to

study such dilute systems. We have used the MS for studying the magnetic ordering in these systems. Mossbauer study of the temperature variation of the sample  $\text{Sb}_{1-x-y}\text{Fe}_x\text{Se}_y$  for  $X=0.002$  and  $Y=0.05$  was also done.

### 3.2 Sample Preparation:

Measured quantities of high Purity Antimony Sb (99.99%), Selenium (99.99%) in powder form and enriched Iron  $^{57}\text{Fe}$  (> 95%) isotope in powder form were used for making  $\text{Sb}_{1-x-y}\text{Fe}_x\text{Se}_y$  alloys, where concentration of Y was taken as 0.03, 0.05, 0.10, 0.20, 0.30. The concentration of the Fe was kept very low ( $X=0.008$ ) so as not to disturb the host lattice. Also the sample with  $X=0.002$  &  $Y=0.05$  was made to study the effect of temperature variation using Mossbauer Spectroscopy. In all these studies enriched  $^{57}\text{Fe}$  isotope was used for sample preparation so that the magnetic ion Fe concentration can be kept in the dilute limit and also get good statistics in the Mossbauer spectrum in reasonably good time. Desired quantities of powder were taken in small quartz ampoules. The ampoules were then evacuated to  $10^{-5}$  torr and sealed. After the encapsulation, the sealed ampoules were shaken to mix the contents thoroughly. All the samples were melted in oxy-butane flame and were kept in melt conditions for 5-10 minutes before quenching to room temperature. The samples were again remelted and this process was repeated several times before they are finally quenched in water. Each of the samples formed shiny globules.

The powd  
should be  
thoroughly  
mixed in  
a mortar  
before.

Approximately 100 mg of samples were ground into a fine powder and mixed with Boron Nitride to make the Mossbauer absorbers. The Boron Nitride ~~here~~

was used to provide proper binding and uniformity of sample for Mossbauer absorbers. The samples were evenly distributed on one mm thin sheet of paper of 1.2 cm diameter.

The remaining part of the samples were used for the characterization of the samples by Hall effect, Magnetoresistance, AC Susceptibility and XRD measurements.

### 3.3 Experimental Results:

#### 3.3.1 Mossbauer Measurements:

Mossbauer spectra of the above samples were recorded using a constant acceleration spectrometer with a line width of 0.28 mm/sec. The calibration of the spectrometer was done using Natural Fe as detailed in Chapter 2 (Fig 2.1). The source used was  $^{57}\text{Co}$  in Rh matrix of strength 25mCi. Typical Mossbauer spectra of all the samples are shown in Fig 3.1 to 3.13. The spectra were least square fitted using Meerwal Program available from which Mossbauer parameters {Quadrupole Splitting (QS), Magnetic Splitting (HMF) and Isomer Shift (IS)} were evaluated and tabulated in Table 1 to 3.

The best fits of the spectra for the samples with  $Y=0.0$  showed a quadrupole doublet of  $QS = 1.28$  (2) mm/sec which corresponds to  $\text{FeSb}_2$  [14] compound phase.

The spectra for the samples with  $Y = 0.03$  show two distinct magnetic sites (HMF) as Site A, Site B and one Quadrupole splitting (QS) as Site C. For  $Y=0.05$  and  $0.10$ , two Magnetic sites Site A, Site B and two Quadrupole sites Site C & Site D are seen

$\text{Sb}_{1-x-y}\text{Fe}_x\text{Se}_y$  System

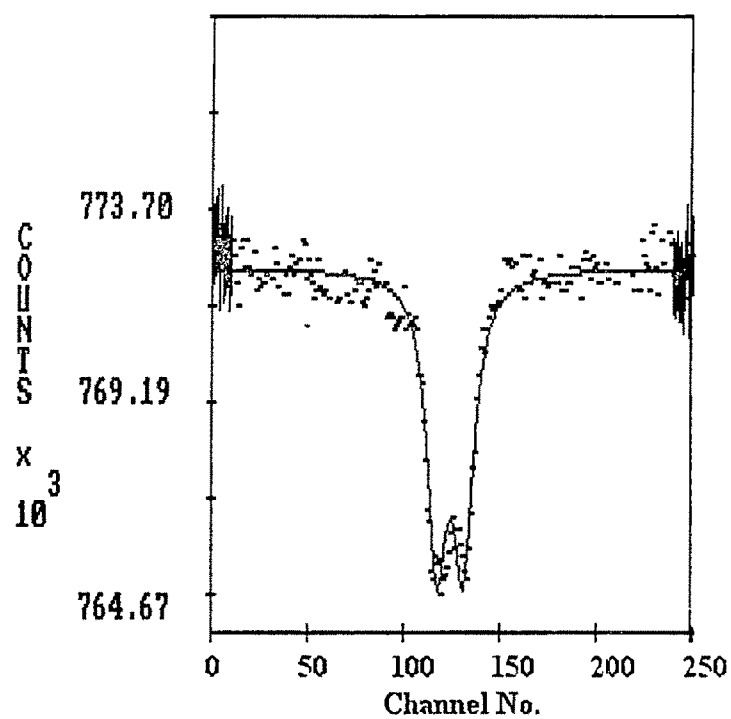


Fig 3.1 Mossbauer Spectra for X=0.008, Y=0.0

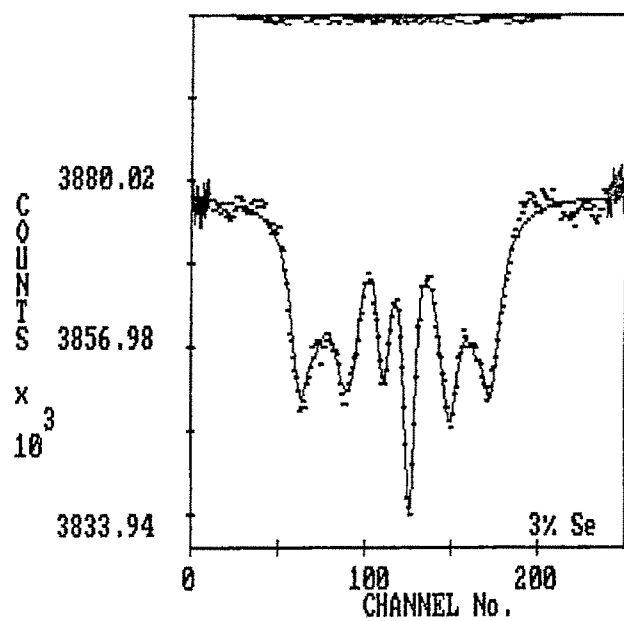


Fig 3.2 Mossbauer Spectra for X=0.008, Y0.03

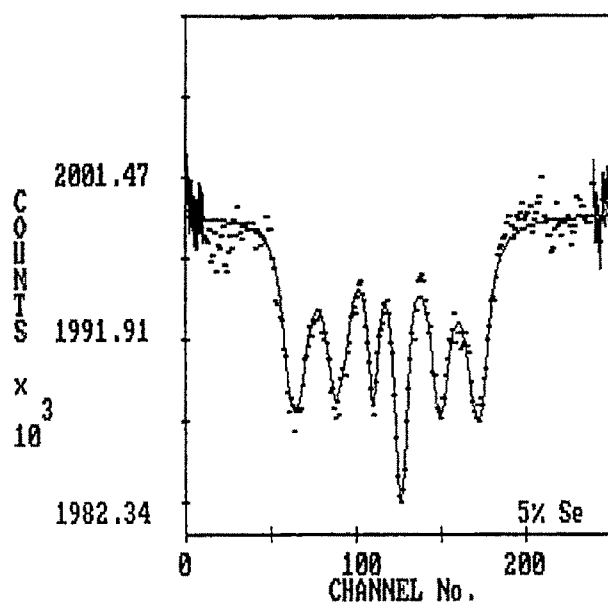


Fig 3.3 Mossbauer Spectra for X=0.008, Y0.05

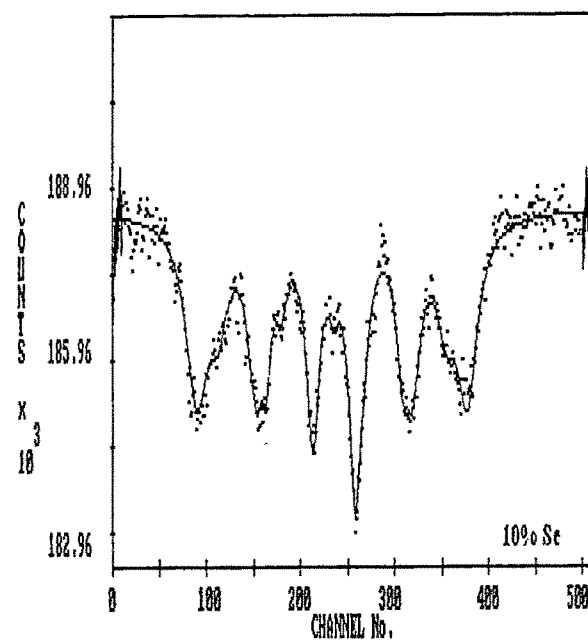


Fig 3.4 Mossbauer spectra for  $X=0.008, Y0.10$



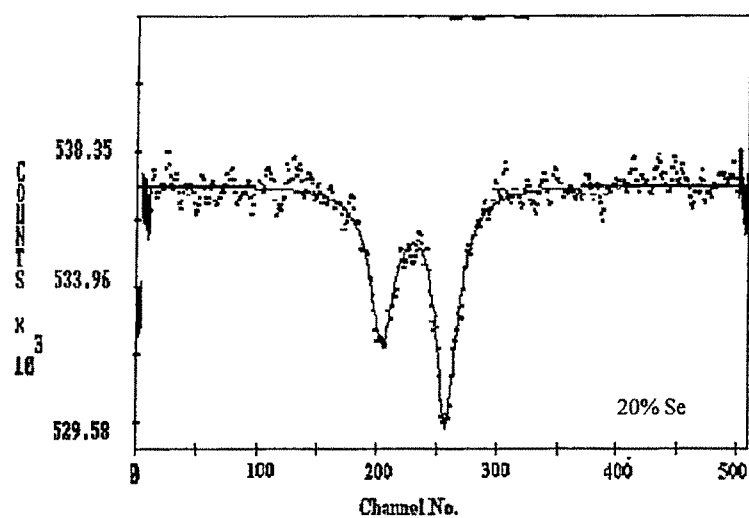


Fig 3.5 Mossbauer spectra for  $X=0.008, Y0.20$

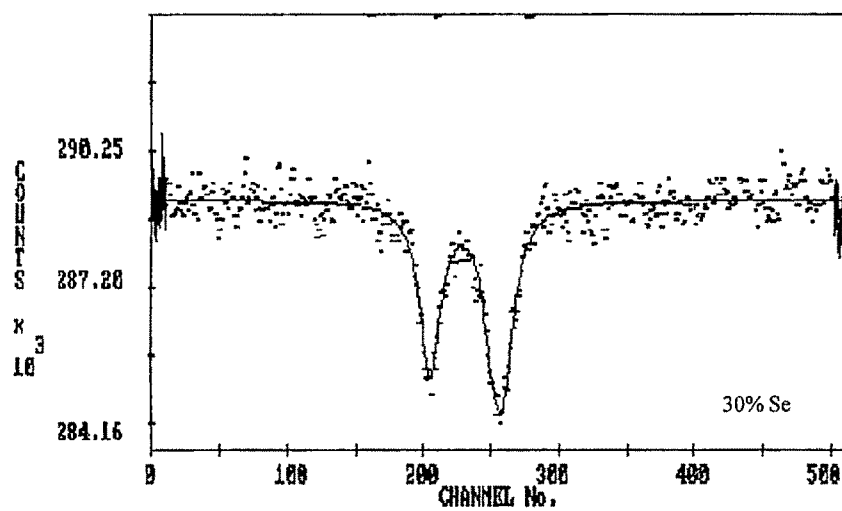
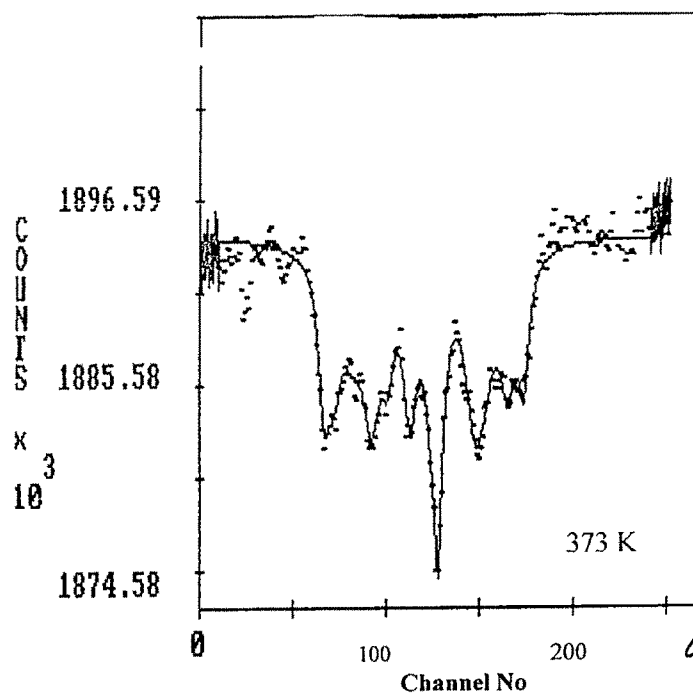


Fig 3.6 Mossbauer spectra for  $X=0.008, Y0.30$

Sample	Value of the Field in (KOe)		QS mm/sec		Isomer shift (mm/sec)				Area under the curve			
	A	B	C	D	A	B	C	D	A	B	C	D
X=.008, Y=0.0	----	-----	1 28 (0.02)	----	----	-----	0 47 (0.02)	----	--	-----	1.00	-----
X= .008,Y=.03	250 8 (1.6)	210 (1.6)	1 25 (.02)	---	0.77 (.05)	0.69 (.07)	0.52 (.04)	---	0.523	0.340	0.137	-----
X=.008,Y=.05	248 (1.6)	211.3 (1.96)	1.28 (.02)	0.53 (.03)	0.77 (.05)	0.69 (.08)	0.52 (.04)	0 28 (0.03)	0.541	0.363	0.08	0.016
X= .008,Y=.10	258.5 (1.6)	218.3 (1.6)	1.29 (.02)	0.51 (.03)	0.74 (.05)	0.69 (.07)	0.33 (.04)	0.26 (0.03)	0 573	0.380	0.023	0.024
X=.008,Y= .20	----	-----	1.45 (0.02)	0.51 (0.02)	-	-----	0 49 (0.04)	0.18 (0.02)	----- --	-----	0.70	0.30
X=.008,Y=.30	----	-----	1.45 (0 02)	0.53 (0.02)	-----	-----	0 52 (0 04)	0.28 (0.03)	-----	-----	0.48	0.52

**Table 1. Mossbauer parameters of sample  $\text{Sb}_{1-x-y}\text{Fe}_x\text{Se}_y$  for X =0.008 and Y=0.03,0.05,0.10,0.20,0.30.**

Temperature variation study of the sample with  $X=0.008, Y=0.05$



← why this spectrum is different from the one in fig 3.3.?  
Temp.

Fig 3.7 shows the Mossbauer spectra of sample  $X=0.008, 0.05$  at 373 K. Is it because of

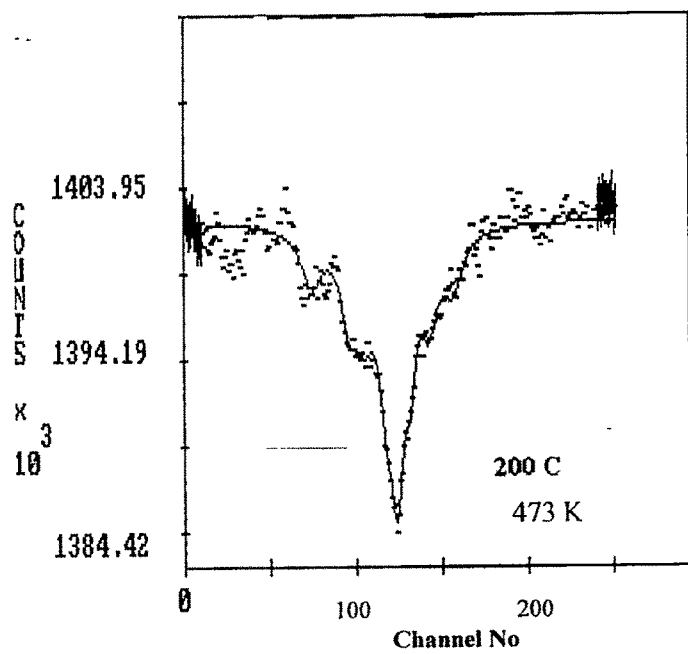


Fig 3.8 shows the Mossbauer spectra of sample  $X=0.008, 0.05$  at 473.

Temperature (K)	Value of the Field in (KOe)		QS mm/sec		Isomer shift (mm/sec)				Area under the curve			
	A	B	C	D	A	B	C	D	A	B	C	D
300	248 (1.6)	211.3 (1.96)	1.28 (.03)	0.53 (.03)	0.77 (.05)	0.69 (.08)	0.52 (.04)	0.28 (0.03)	0.541	0.363	0.08	0.016
373	247 (1.06)	216 (1.5)	1.30 (.03)	0.53 (0.03)	0.67 (.05)	0.69 (.07)	0.49 (.04)	0.23 (0.03)	0.265	0.546	0.100	0.089
473	190 (3.7)	—	1.28 (.03)	0.53 (.03)	0.76 (.05)	—	0.52 (.04)	0.28	0.510	—	0.249	0.241

Table 2. Mossbauer data of Temperature variation of sample with X=0.008, Y0.05

The QS of Site C was calculated as 1.28 (2) mm/sec which remained constant for all the three concentrations of Se. The QS and Isomer shift (IS) of this site indicates the formation of FeSb<sub>2</sub> [14] compound phase in the system.

The QS of Site D was evaluated as 0.51 (2) mm/sec which corresponds to Sb<sub>2</sub>Se<sub>3</sub> phase formation in the system.

The Site B has the HMF= 220 (2) KOe and the IS as 0.69 mm/sec for all concentrations of Se. Also the population of site increased marginally with increase in concentration of Se upto Y= 0.10. These values match well with one phase of Fe<sub>7</sub>Se<sub>8</sub> [15]. The earlier studies on Fe<sub>7</sub>Se<sub>8</sub> show three possible magnetic sites of Fe<sub>7</sub>Se<sub>8</sub> having HMF values as 237, 193 and 172 KOe and IS 0.70, 0.67 and 0.65 mm/sec respectively. This compound at room temperature is ferrimagnetic in nature and has the curie temperature  $T_c = 443$  K. Thus Site B could be attributed to one of the magnetic sites of Fe<sub>7</sub>Se<sub>8</sub> phase in the system. To support this argument, temperature variation of one of the sample (Y=0.05), was done at RT, 373, 473. Mossbauer spectra of the sample at these temperatures are shown in Fig 3.2, 3.8-3.9. The corresponding Mossbauer parameters are given in Table 3. The results clearly show that Site B disappears at 473 K temperature, thereby indicating that the curie temperature of this site is below 473K. Hence, it supports the argument of formation of Fe<sub>7</sub>Se<sub>8</sub> phase in the system.

The HMF value of Site A was found to be 250KOe and IS as 0.77 mm/sec. It is observed that as the Se concentration is increased the population of Site A also

increases. Since the Mossbauer parameter of this site does not match with any other compound phases of Fe-Se or Fe-Sb, the probability of such combinations can be ruled out.

Sb is a semimetal and has a very small <sup>d</sup>band gap of less than 0.1 eV at RT. It is known that Se has higher valency states (+6) than the Fe (+3) & Sb (+3,+5). ←

Therefore, Se is likely to contribute charge carriers (electrons) in the system, thereby behaving as a donor in the matrix. Also there is large electronegativity difference between Fe (1.8) and Se (2.4). So, Se is expected to be strongly attracted towards Fe and thereby forming Fe-Se pairs, with consequent breaking of covalent bonds between Fe and Sb. This may be responsible for forming Fe local moments through sp-d exchange between Se and Fe ions.. Further with increase in the Se concentration conduction electron densities are expected to increase in the system. These conduction electrons could be responsible for polarizing the local moments of Fe and giving rise to the observed magnetic order in system. Thus, the magnetic interaction at this site A can be understood with RKKY type of interaction. The decrease in the population of the quadrupole site C with simultaneous increase in the population of site A and B as Se concentration increases, indicates that in Sb the Se-Fe pair formation is more probable than forming the FeSb<sub>2</sub> (Site C) compound phase. Thus it appears that a ternary alloy of Sb-Fe-Se is responsible for the magnetic site in the system. The increase in charge carrier densities with increase in Se concentration was observed through Hall measurements as discussed later.

On increasing the Se concentration to  $Y=0.20$  and  $0.30$  the two magnetic sites disappeared and the two quadrupole sites Site C and Site D only were observed. Fig 3.5-3.8 shows the spectra and Table 2 gives the analyzed parameters of it. The values of QS at Site C and Site D were evaluated as  $1.45$  &  $0.51$  mm/sec respectively. Absence of any magnetic site at higher concentration of Se can be due to the formation of compounds like SbSe and  $Sb_2Se_3$  phases. Here the  $QS = 0.51$  corresponds to  $Sb_2Se_3$  phase formation [16], which is supported by the results discussed in chapter 4. Also the XRD data shows clear phase of  $Sb_2Se_3$  at higher concentration of Se. The second site C can be attributed ~~due~~ to  $FeSb_2$  /SbSe. The XRD data has few unidentified peaks which may be due to the formation of SbSe compound for which no data is available in the literature. We are now trying to make a complete study of this SbSe compound separately.

#### Temperature variation of $Fe_{0.002}Sb_{0.948}Se_{0.05}$ sample.

In order to avoid the formation of nonmagnetic compound phase between Fe and Sb, the concentration of Fe was kept low ( $X=0.002$ ) and the Se concentration was kept as  $Y=0.05$ . The Mossbauer spectra were taken at RT, 373K, 473K, 573K and Back at RT. At this concentration of Fe the spectra do not show the QS of  $FeSb_2$ . Fig 3.9-3.13 shows the corresponding spectra and the parameters evaluated from the analysis of the spectra are given in Table 2. The spectra showed two magnetic sites as Site A & Site B and one quadrupole site as Site C.

Temperature variation study of the sample  $\text{Fe}_{0.002}\text{Sb}_{0.948}\text{Se}_{0.05}$

Sample X= 0.002, Y=0.05

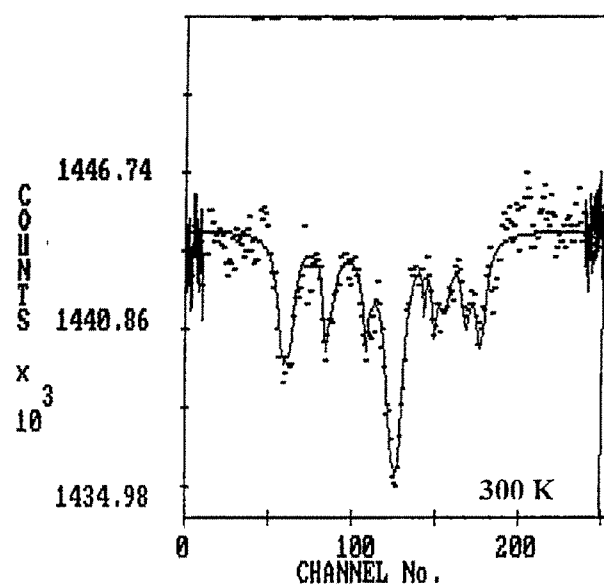


Fig 3.9 Room temperature Mossbauer spectra

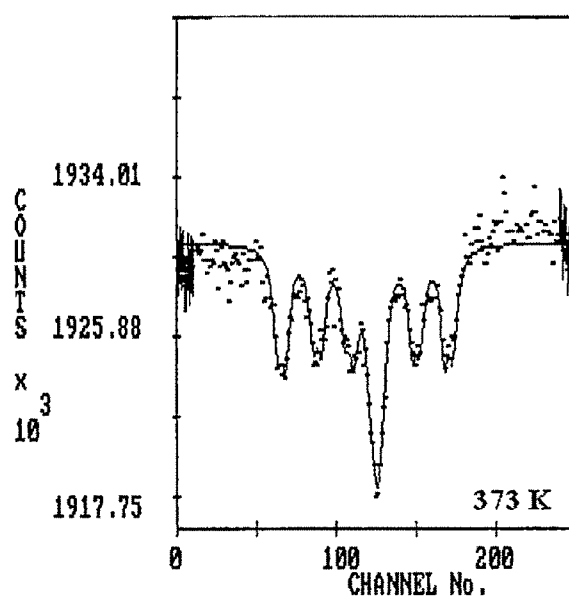


Fig 3.10 Mossbauer Spectra at 373K



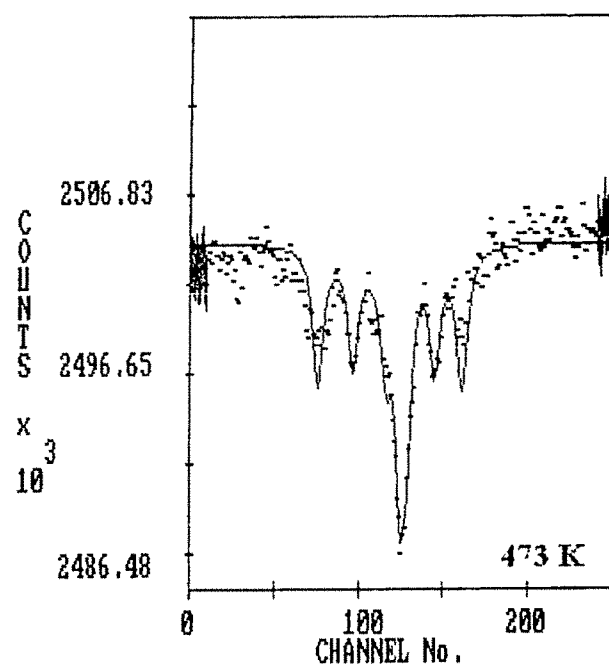


Fig 3.11 Mossbauer Spectra at 473K

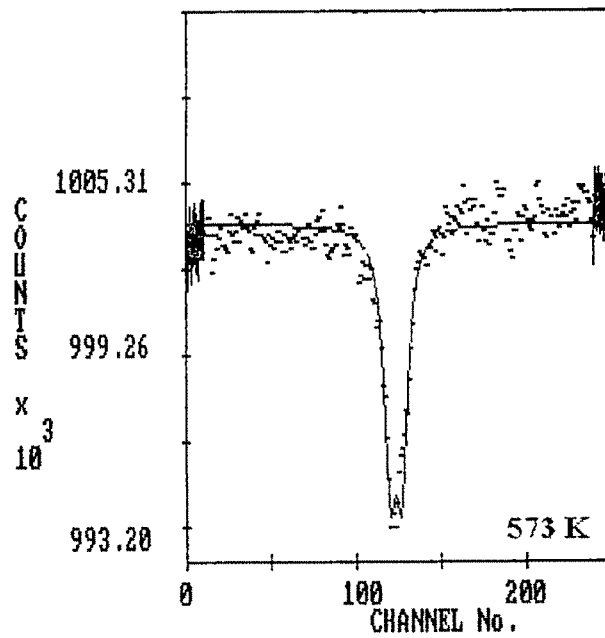


Fig 3.12 Mossbauer Spectra at 573K

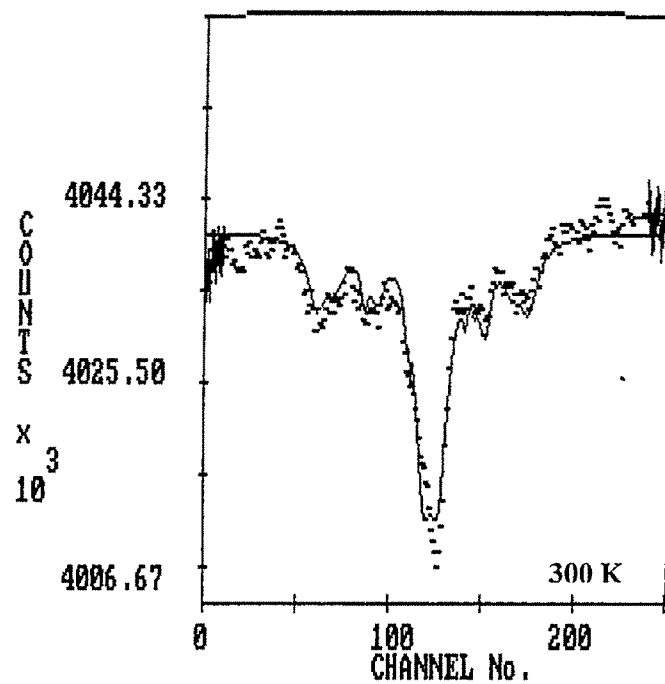


Fig 3.13 Room temperature Mossbauer Spectra after temperature variation study

Temperature (K)	Magnetic Field in K.Oersted		Quadrupole Interaction m/sec	Isomer shift			Fractional Area		
	A	B		A	B	C	A	B	C
300	265.7 (1.6)	236.8 (1.69)	0.51 (0.02)	0.76 (0.01)	0.68 (0.01)	0.28 (0.01)	0.522	0.361	0.117
373	256.39 (1.69)	227.9 (1.73)	0.53 (0.02)	0.76 (0.01)	0.69 (0.01)	0.17 (0.01)	0.424	0.410	0.151
473	198.27 (1.53)	-	0.53 (0.02)	0.60 (0.01)	-	0.09 (0.01)	0.786	-	0.214
573	-	-	0.51 (0.02)	-	-	0.06 (0.01)	-	-	1.000
300 Back	268 (1.02)	223 (1.76)	0.51 (0.01)	0.43 (0.02)	0.47 (0.01)	0.32 (0.02)	0.220	0.25	0.531

**Table 3. Mossbauer parameters of the temperature variation of sample with X=0.002, Y0.05**

The QS of Site C was found to be 0.51 mm/sec, which corresponds to  $\text{Sb}_2\text{Se}_3$  phase. Hence the formation of  $\text{Sb}_2\text{Se}_3$  seems unavoidable even at 0.05 concentration of Se. But the formation of  $\text{FeSb}_2$  could be avoided.

Site B in this sample is due to ferrimagnetic phase  $\text{Fe}_7\text{Se}_8$  as observed earlier in higher concentration of Fe. This phase appears to be vanishing at 473 K, thereby supporting the evidence of it. However, the second magnetic site A disappears at 573K, which reveals that curie temperature of it is between 473K and 573K. The cause of Site A is already being understood as due to RKKY type of magnetic interaction. However, on recording the spectra back at room temperature showed the reappearance of all the three sites, but absorption of the magnetic sites reduced as seen in the Fig 3.5 which may be due to the formation of more non magnetic compound phases ( $\text{Sb}_2\text{Se}_3$ ) during temperature variation study.

This can be confirmed from the increase in the relative population of  $\text{Sb}_2\text{Se}_3$  from the fitted data.

→ This must also be checked by comparing the x-ray data at the two situations.

### 3.3.2 Hall Measurements

The Hall measurements were carried out on the samples with Se concentrations as 0.00, 0.008, 0.03, 0.05 and 0.20. Table 4 gives the data of same. At all the concentrations, the samples showed n-type nature. It is observed that as the Se concentration is increased upto 0.05, charge carriers concentration (electrons in this case) increases from  $4.2 \times 10^{19}$  to  $1.14 \times 10^{21}$  and the conductivity of the system increases from  $759.9 \text{ (ohm-cm)}^{-1}$  to

3215.8 (ohm-cm)<sup>-1</sup>. We have seen that upto 0.05 concentration of Se, Mossbauer study shows a magnetic interaction at room temperature. However at higher concentrations of Se (Y=0.20), the carrier concentration decreases drastically by an order of 10<sup>6</sup> with respect to 0.05 concentration of Se. This may be due to the formation of compound phase between Sb and Se, thereby decreasing the itinerant charge carrier density in this system. Through Mossbauer study we have observed only quadrupole site of Sb<sub>2</sub>Se<sub>3</sub> and FeSb<sub>2</sub>, which supports our argument. Hence the results of the Hall measurements confirm that the system behaves as an n type semiconductor and the charge carrier densities increase upto 0.10 Se concentration give support to the hypothesis with which we started these measurements viz the magnetic order in the sample can be brought about through the mediation of charge carriers introduced by the doping of an anion impurity (Se) in Sb matrix containing very dilute Fe.

**Table 4. Hall Measurement of Sb<sub>1-x-y</sub> Fe<sub>x</sub>Se<sub>y</sub> (X=0.008)**

Se concentration (y)	Hall concentration Rh	Carrier concentration (n)	Mobility Cm <sup>2</sup> /v.s	Conductivity (Ohm-cm) <sup>-1</sup>
0.0	0.15	4.2 x 10 <sup>19</sup>	----	----
0.008	0.02	2.95 x 10 <sup>20</sup>	16.1	759.92
0.02	0.013	4.42 x 10 <sup>20</sup>	12.6	891.07
0.05	0.0054	1.142 x 10 <sup>21</sup>	17.6	3215.87
0.20	0.11	5.67 x 10 <sup>19</sup>	38.9	352.9
0.50	2976	2.1 x 10 <sup>15</sup>	77.1	0.0259

### 3.3.3 X-Ray Diffraction Studies

Fig 3.14 shows the XRD spectra of Sb sample and Fig 3.15 -3.17 shows the XRD spectra of samples for Y=0, 0.03 and 0.20 concentration of Se. These samples were prepared by spreading out the powder on glass slide. Grease was used to fix the sample on glass plate. All the spectra were recorded at room temperature by a standard X-Ray Diffractometer using Cu-K $\alpha$  radiation ( $\lambda = 1.54 \text{ \AA}$ ). The  $2\theta$  values and relative intensities ( $I/I_0$ ) of the samples were compared with JCPDS cards of the data available for the standard phases possible.

For Y= 0 concentration of Se, the  $2\theta$  values indicate the peaks of Sb. It is obvious that as the Fe concentration in the system is very low ( $X=0.008$ ), the corresponding Fe based compound phases won't be showing up in the XRD pattern. On increase in the concentration of Se to 0.03, the pattern showed Sb peaks and small amount of Sb<sub>2</sub>Se<sub>3</sub> phase formation in the system. With increase in concentration of Se to Y=0.20, the formation of Sb<sub>2</sub>Se<sub>3</sub> also increased and became more prominent. However, the residual peaks of unreacted Se were also found in the system at such a higher concentration and a few unidentified peaks which we think are related to the formation of SbSe compound. In the JCPDS cards in the literature, no data is available for SbSe compound. From the results of XRD it can be concluded that at higher concentration of Se the chances of compound phase increases thereby reducing the carrier densities in the system. This was also confirmed by Hall measurements which showed drastic decrease in carrier concentrations at higher concentration of Se.

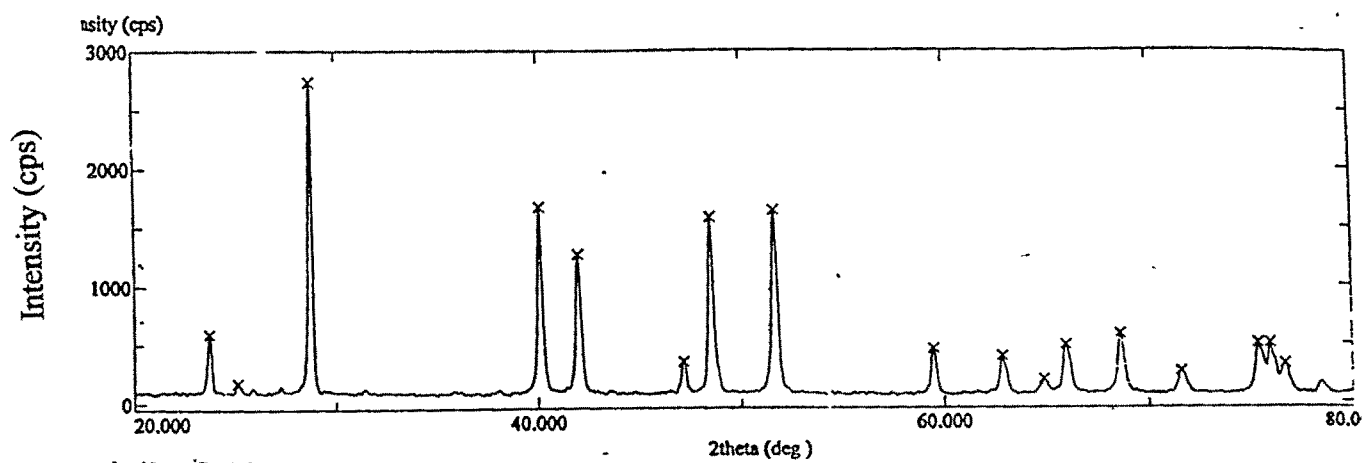


Fig 3.14 XRD spectra of Sb sample

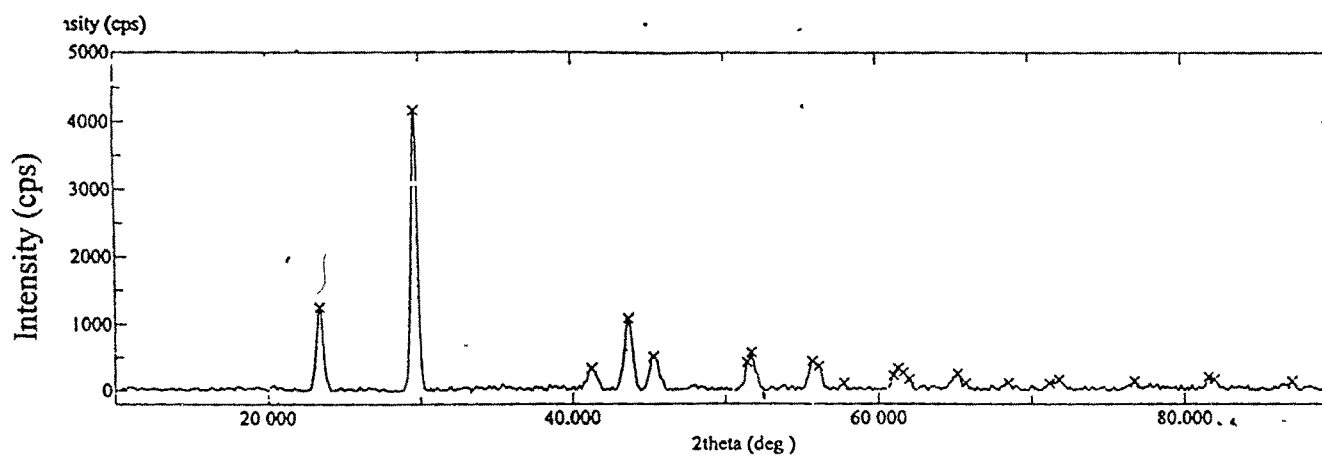


Fig 3.15 XRD spectra of Se sample

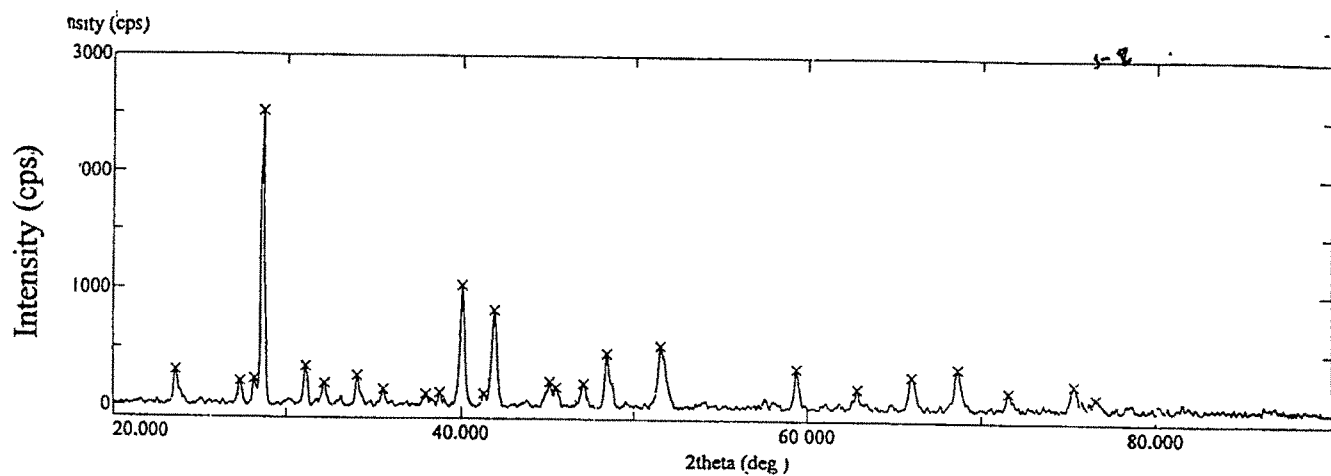


Fig 3.16 XRD spectra of sample Y=0.03

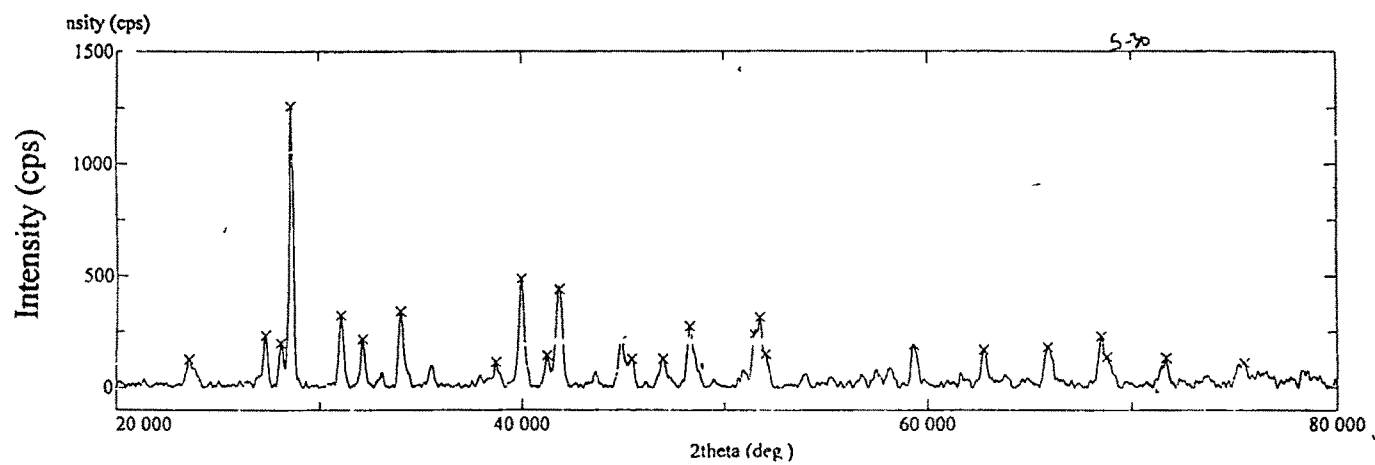


Fig 3.17 XRD spectra of sample Y=0.20



### 3.3.4 Magnetoresistance measurements:

Magnetoresistance (MR) measurements were done for the samples  $Sb_{1-x-y}Fe_xSe_y$  ( $Y=0.03, 0.10$ ) at 5K, 50K, 150K and 300K temperatures. The magnetic field applied to the samples was upto  $\pm 80$ KOe. The plots of MR vs Magnetic Field and Resistance vs temperature (at 0 & 9T fields) are shown in Fig 3.18-3.21.

Figures indicate that the system has positive response to magnetic field at all the temperatures with the hysteresis behavior. The magnitude of MR was found to be increasing with decreasing the temperature for all the three concentrations. At 5K these samples showed rise of 200% of MR ratio in  $Sb_{0.962}Fe_{0.008}Se_{0.03}$  and 100% in  $Sb_{0.892}Fe_{0.008}Se_{0.10}$ . The behavior of samples with  $Y=0.03$  & 0.10 concentrations was found to be similar.

The Resistance vs temperature plots of the sample shows strong dependence of resistance with temperature. The resistance at 0 & 9T applied field of the samples ?  
( $Y=0.03, 0.10$ ) showed sharp decrease with decrease in temperature. For  $Y=0.03$ ,

the resistance reaches to a minimum at  $\sim 70$ K with a value of 1.2 mohm after which there is steep increase in resistance with further decrease in temperature.

This is true only with field

Needs better explanation

This low residual resistivity implies that the electronic conduction is mainly due to electron-electron scattering [17]. For  $Y=0.10$ , the resistance response to temperature was similar like in  $Y=0.03$ . However, the steep transition at low temperature was not observed at  $Y=0.10$  concentration of Se, thereby indicating that as Se concentration increases the magnetic response of the sample decreases.

This sharp transition from metal to semiconducting phase is quite unusual in ?

such systems.

The positive MR can be well understood here as an increase in spin-dependent scattering in the presence of the magnetic field. The spin splitting can be caused by sp-d exchange interaction between the conducting hybridized sp-band electrons of Se and the localized d-electron spins of Fe ions and the rise of the Fermi level in the majority subband [18]. Thus the exchange enhances spin splitting, leading to an unusual large positive MR.

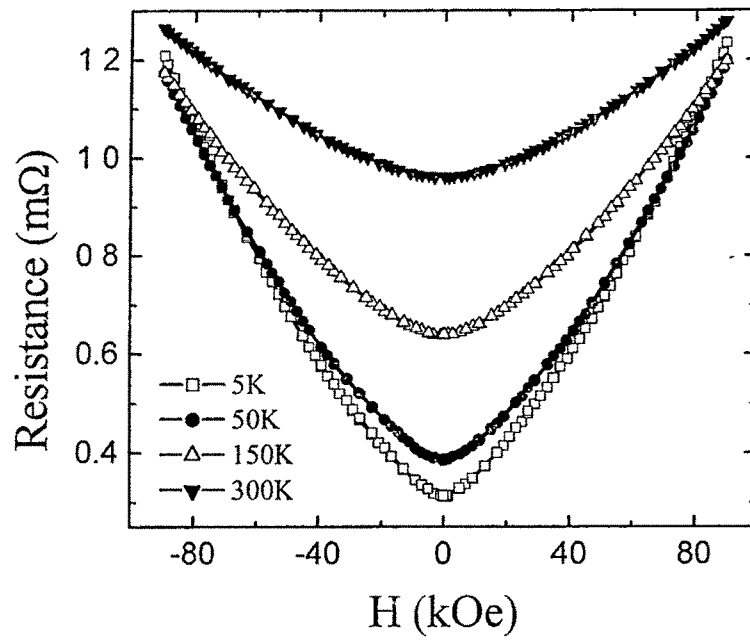


Fig 3.21 Magnetoresistance vs Magnetic Field of a sample with X=0.008, Y=0.03

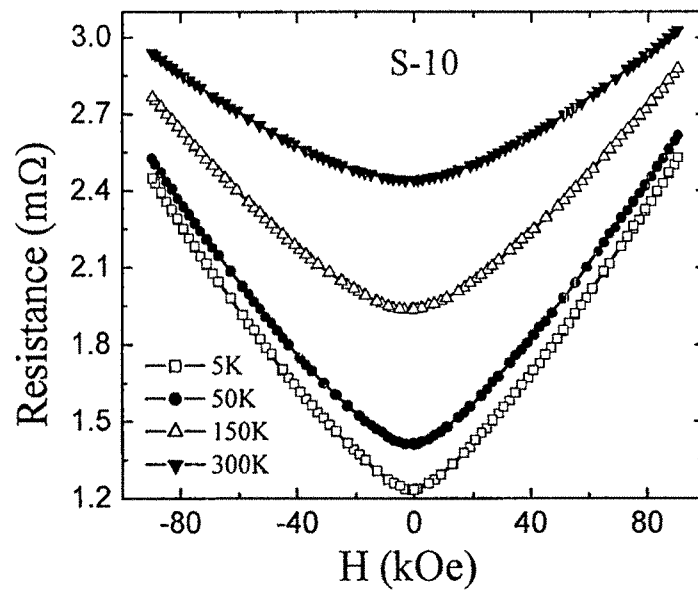


Fig 3.21 Magnetoresistance vs Magnetic Field of a sample with X=0.008, Y=0.10

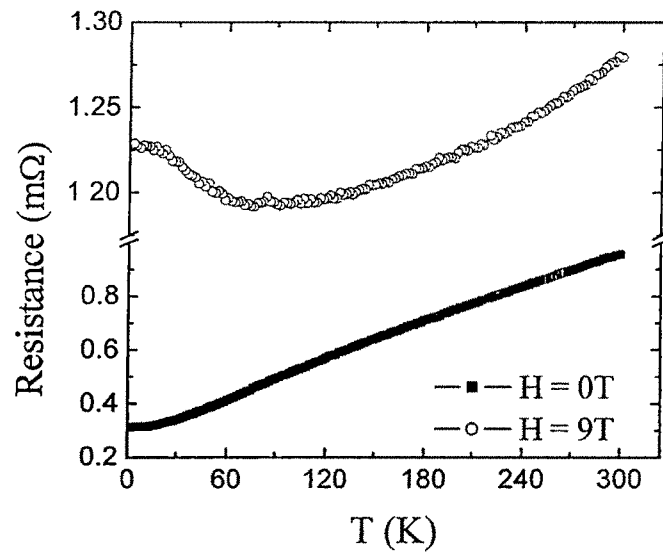


Fig 3.21 Magnetoresistance vs Temperature plot of a sample with  $X=0.008$ ,  $Y=0.03$

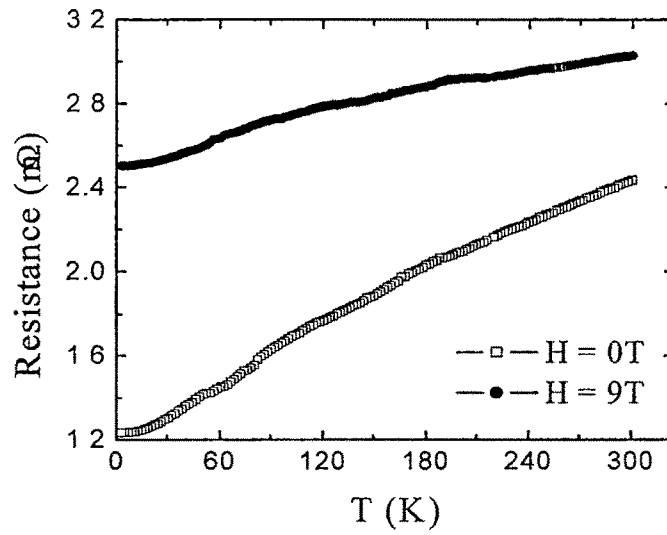


Fig 3.21 Magnetoresistance vs Temperature plot of a sample with  $X=0.008$ ,  $Y=0.10$

### 3.3.5 AC Susceptibility measurements:

Fig 3.23-24 shows AC susceptibility vs temperature plot of samples for  $Y=0.05, 0.10$  at the applied frequency 111.11 Hz and 80A/m magnetic field. In both the plots there is a cusp at 120K temperature. On plotting  $\chi^{-1}$  vs T, one can have convex curvature with negative intercept of the linear extrapolation of high temperature portion of  $\chi^{-1}(T)$ . This indicates that the transition could be ferrimagnetic due to the secondary phases in the system [19]. The cause of secondary phase is already being identified as due to the formation of  $Fe_7Se_8$  through Mossbauer spectroscopy.

However the indication of cusp in the system may probably be feature of a spin glass, which can only be confirmed by studying the frequency dependence of AC Susceptibility vs Temperature.

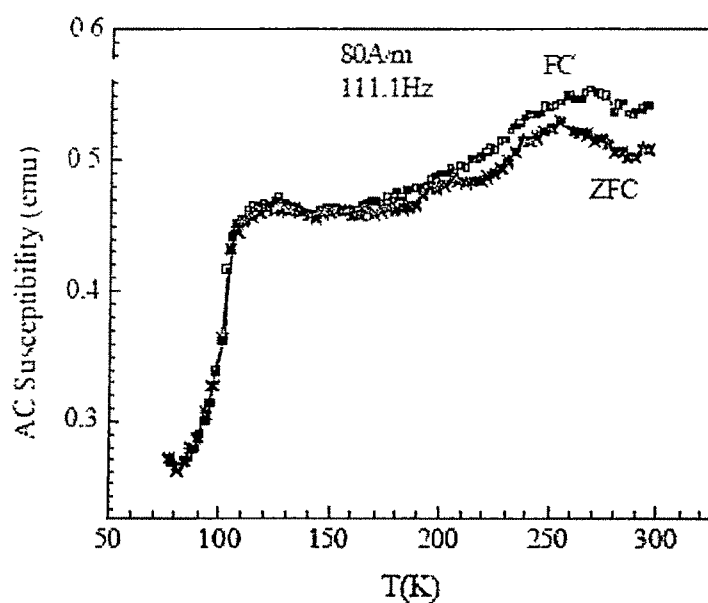


Fig 3.23 AC Susceptibility plot of Sample with X=0.008, Y=0.05

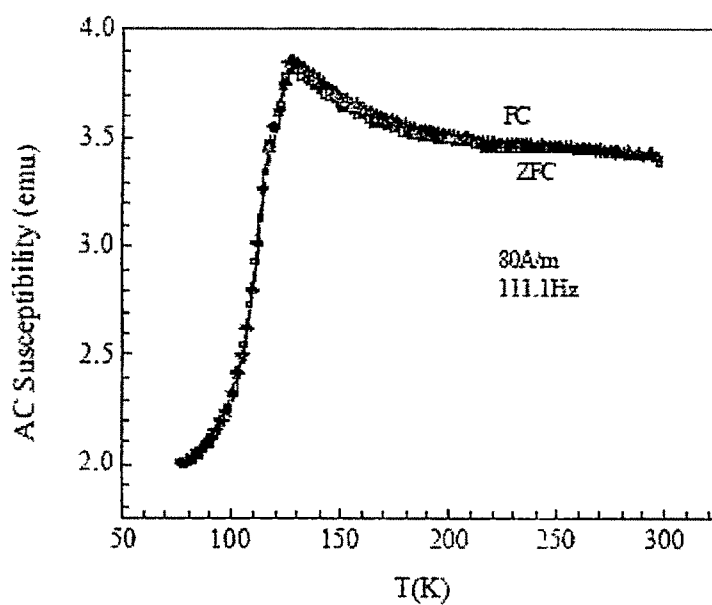


Fig 3.23 AC Susceptibility plot of Sample with X=0.008, Y=0.10

### 3.4 Summary

In this chapter, we have discussed the magnetic properties of  $\text{Sb}_{1-x-y}\text{Fe}_x\text{Se}_y$  ( $x=0.008$ ,  $y=0.03, 0.05, 0.10, 0.20$  and  $0.30$ ) alloys. The alloy was found to be magnetic upto  $y=0.10$  concentration of Se with two distinct sites observed. One of the magnetic sites was attributed to  $\text{Fe}_7\text{Se}_8$  and another due to the sp-d exchange between Se-Fe and RKKY interaction with spin-spin coupling mediated by the Fermi sea of conduction electrons which could lead to a magnetically ordered system. The positive response to magnetic field and enhancement in magnitude of field at low temperatures observed in magnetoresistance measurements indicates the effect of sp-d exchange interaction and conduction electrons mediated (RKKY) mechanism. The evidence for bringing charge carriers of the n type into the system was confirmed through Hall measurements. Above  $y=0.10$  concentration of Se, there was a sharp decrease in charge carrier concentration (from hall studies) and Mossbauer spectra showed only quadrupole site, thereby indicating the nonmagnetic compound phase formation. The XRD data points to  $\text{Sb}_2\text{Se}_3$  and  $\text{SbSe}$  phase formations at higher concentration of Se.

Efforts are being made to find different methods of preparation primarily to avoid the formation of the  $\text{Fe}_7\text{Se}_8$  magnetic phase and as far as possible also non magnetic phases in these samples.

Thin film studies of these samples are also being attempted.

## References:

1. Dilute Magnetic Semiconductors, M. Jain (Eds), World Sci., Singapore, 1991
2. J.K. Furdyna, T. Kossut, Dilute Magnetic Semiconductors, Vol-25 of Semiconductors and Semimetals, Academic Press, Boston, 1988.
3. M. Averours, M. Balkanski, Semimagnetic Semiconductors and Dilute Magnetic Semiconductors, Plenum Press, London, 1991.
4. R.N. Bhatt, Mona Berciu, Malcolm P. Kennett, and Xin Wan, Dilute Magnetic Semiconductors in the low carrier density regime, Journal of Superconductivity: Incorporating Novel Magnetism, Vol. 15, No. 1, February 2002. *Page!*
5. H. Ohno, Science 281, 951 (1998) ~~951~~
6. K. Ueda, H. Tabata and T. Kawai, Appl. Phys. Lett. 79 (2001) 988.
7. M.L. Reed, E.L. Masry, H.H. Stadelmaier, M.K. Rytums, M.J. Reed, C.A. Parker, J.C. Roberts and S.M. Bedair, Appl. Phys. Lett. 79 (2001) 3473.
8. Y. Matsumoto et al. Science 291 (2001) 854
9. G.A. Medvedkin, T. Ishibashi, T. Nishi, K. Hayata, Y. Hasegawa and K. Sato, Jpn. J. Appl. Phys., Part 2 39 (2000) L949
10. S. Choi, G.B. Cha, S.C. Hong, S. Cho, Y. Kim, J.B. Ketterson, S.Y. Jeong and G.C. Yi, Solid State Commun. 122 (2002) 165.
11. S. Cho et al., Phys. Rev. Lett. 88 (2002) 257203.
12. F. Matsukura, H. Ohno, A. Shen and Y. Sugawara, Phys. Rev. B 57, R2037 (1998).
13. T. Dietl, A. Haury and Y. Merle d'Aubigny, Phys. Rev. B 55, R3347 (1997).



14. Y.K.Sharma, Hyp.Int., 28,1-4,1013-1016,1986

*have contributed in the front*

15. H.N.Oak, S.W.Lee., Phys.Rev. B. 8,4267, 1973.

16. D.R.S.Somayajulu, Mukesh Chawda, Narendra Patel, K.C.Sebastian and

M.Sarkar., Solid State Physics, India. 2002

P.

17. Y.D.Park, J.D.Lim, K.S.Suh, S.B.Shim, J.S.Lee, C.R.Abernathy, S.J.Pearton,

Y.S.Kim, Z.G.Khim and R.G.Wilson., Phys. Rev. B., 68 (2003) 68.

18. M.Sawicki, T.Dietl, J.Kossut, J.Igalson, T.Wojtowicz and W. Plesiewicz.,

Phys. Rev. Lett. , 56 (1986)508

19. S.Chikazumi, Physics of Magnetism (wiley, New York, 1964), p.9